DETERMINATION OF LOW PRESSURE GAS INJECTOR VALVE FLOW FACTOR

Dariusz Szpica
Faculty of Mechanical Engineering, Bialystok University of Technology,
45C Wiejska Str., 15-351 Bialystok, Poland;
d.szpica@pb.edu.pl

Abstract. During the time when exhaust toxicity effects have an important role in the means of transport, engines are very often converted to be supplied by alternative fuel. The most popular alternative fuels used in transport vehicle engines are liquefied petroleum gas and compressed natural gas. In both cases, the fuel dosage component is the low pressure gas injector. There are many design constructions for these injectors, i.e. plunger, plate or membrane. The most popular are plunger injectors. In the course of mathematical modelling of the combustion engine fuel supply system operation, it is necessity, among other things, to determine the flow parameters of components, mainly the values of flow factors. The article presents the results of plunger injector experimental flow tests at various opening levels. For this purpose, the original laboratory stand and flow meter were used. An original method for determining the cross-section flow area for a plunger valve has been proposed. The determined coefficient is universal and it is used in the case of plunger injectors. Tests at varying degrees of opening are static, because the flow is steady and the plunger is stationary. An attempt was made to validate the results of static tests under dynamic conditions. For this purpose, our own research method was used, consisting of emptying the tank with a pressure sensor mounted under dynamic injector operation. The results of measurements are flow pressure graphs. They reflect the cyclical operation of the injector. In the final stage experimental and model waveforms were compared (mean absolute percentage error did not exceed 0.5%). Theoretical values were calculated on the basis of a simplified flow model, taking into account the coefficient and field of free flow from static tests. As a result, the applicability of the parameters obtained from static tests for dynamic applications was assessed.

Keywords: mechanical engineering, gas injector, research.

Introduction

From 2021, phased in from 2020, the EU fleet-wide average emission target for new cars will be 95 $gCO_2 \cdot km^{-1}$. This emission level corresponds to a fuel consumption of around 4.1 $l \cdot (100\ km)^{-1}$ of petrol or 3.6 $l \cdot (100\ km)^{-1}$ of diesel [1]. The driving tests according to which the vehicle emissions are assessed have also been modernized: the World Harmonized Light Vehicle Test Procedure (WLTP) [2] and the Real Driving Emissions (RDE) [3]. There are ongoing works on the emission limits for the engines of the machines and non-road vehicles [4; 5]. The latest emission restrictions decrease the possibility to correct the combustion process [6-11]. A certain solution to this situation is use of fuels with reduced carbon content [12-15] or systems supporting combustion engines (hybrid drives) [16; 17]. Electric drives [18], pneumatic drives [19], or H_2 fuel [20; 21] are becoming increasingly popular.

One of the most popular sources of alternative power supply on the EU roads is the liquefied petroleum gas (LPG) vapour injection system [12]. The component element of this type of power supply is a low pressure gas-phase injector. There are various design solutions of the injectors, where the valve element can be a plunger, plate, flap and membrane. The most common are plunger injectors, which differ from each other in design details. In the majority of cases, the movement of the piston is performed by an electromagnetic system. Researches are being conducted on the use of multilayer materials, piezoelectric materials [22-25] and assessment of the wear processes [26; 27].

The determination of the flow characteristics of pneumatic elements is necessary for building of various types of systems or mathematical modelling. For this purpose, standardised methods are used [28], primarily regarding the determination of sound conductivity and critical pressure ratio according to ISO 6358, dimensional coefficients according to ANSI/(NFPA) T3.21.3 or PN-EN 60534-4 [29]. The presented methods specify a pressure ratio during the test at a level of 6.5±0.2e5 Pa, which is situated outside the low pressure gas injector operating range of (1-1.2)e5 Pa. In addition, the previously presented testing methods involve a defined opening of the test element, which in the case of a low pressure gas injector is not adequate, as it is a component with impulse operation. The gas injector manufacturers usually specify the maximum flow in the technical specifications, however, since some time, they also make the flow value dependent on the injection time [30]. The list of research methods of injectors of various fuels can be found in [31]. In determining the flow

characteristics, the evaluated parameters are usually the mass and volumetric flow rate. The various types of the flow coefficient or factor are also determined, which are the basis for calculating the mass or volumetric flow rate. The general classification of the research methods are the direct and the indirect methods [29]. In the direct tests, the volumetric air mass or volumetric flow rate flowing through the tested element under specified supply conditions is measured. Indirect tests, in turn, are the determination of the significant parameters that are used in the standardized procedures or own methods of the numerical identification. As an example, the registration of the pressure changes in the tanks acting as flow meters can be done [29]. Basing on this, the flow factor can be determined using the adopted mathematical model [32]. As it was demonstrated in [33], the differentiation of the flow function at the identification of throughputs has an impact on the final result. There are several indirect methods and these are mainly the tank methods, in which the tanks are filled or emptied while flowing through the test element. The following methods can be distinguished: emptying the tank to the atmosphere [32], flow from the tank to the tank [29; 33; 34], filling the tank from the atmosphere [35]. The advantage of the tank methods is shorter testing time and lower air consumption. The usage of the pressure transmitters, instead of the expensive flow meters, also appeals for these methods. However, the necessity of using specific software which is able to solve differential equations proves the disadvantage of these methods. As the research [33; 34] has demonstrated, it is possible to obtain a high degree of compliance of the theoretical courses with the reality. An unquestionable advantage of the tank methods is the evaluation of the flow parameters in a determined pressure range, rather than as it is in the standardized methods, at one point.

The purpose of this study is to determine the flow factor value at flow through the valve element of the low pressure gas injector.

Materials and methods

The object of the analysis was the Valtek Rail Type 30 low pressure gas injector (Fig. 1). The injector represents a group of the plunger injectors. At rest, without the power supply, the plunger *1* is pressed by the spring *2* to corps *3* using the limiter *4*. By powering the coil *5* and closing the electromagnetic circuit jumper *6,* the plunger *1* starts moving into the pilot *7* and gas flows from the inlet nozzle *8* to the outlet nozzle *9*. The operation of the injector is impulsive and depends on the power supply conditions.

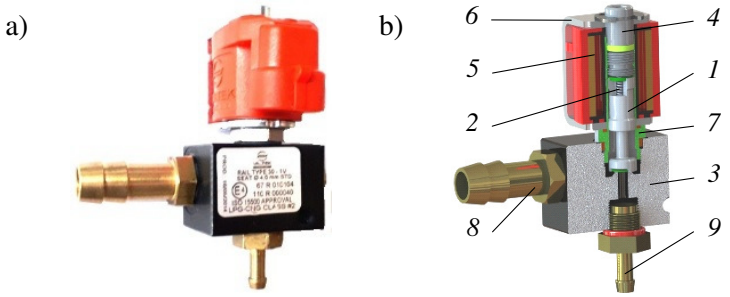

Fig. 1. **Valtek Rail Typ 30 gas injector:** a – photo; b – *CAD* model (description in the main text)

Basic technical data of the tested injectors Valtek are presented in Table 1.

Table 1

Basic technical data of the Valtek Rail Typ 30 gas injector [30]

Parameter	Unit	Value
Coil resistance	Ω	3
Plunger displacement	mm	0.4
Nozzle size	mm	min. 1.5/max. 3.5
Opening time	ms	3.3
Closing time	ms	2.2
Max working pressure	Pa	4.5e5
Operating temperature	ºC	–20-120
Operating voltage range	VDC	12

The test stand (Fig. 2) was used to determine the flow characteristics of the gas injectors [32]. In this case, two types of tests were carried out. In both variants, the compressed air from the air supply *1* was supplied through the air preparation system *2* to the buffer tank *3* and further to the electro valve control system *4*. In the static measurements, the electro valve *4* was open and the air flowed through the flow meter *6* to the research injector *7,* in which the valve opening value was changed every time in continuous flow. In the dynamic measurements, following opening the electro valve *4* the air tank *5* equipped with a pressure gauge or the pressure convertor *8* was filling. Upon filling the air tank *5* electro valve *4* was closing the air supply. The cyclic operation of the injector *7* was started, as a result of which the air tank *5* was cyclically emptied. The pressure recorded as a result of emptying the air tank *5* was used for dynamic validation.

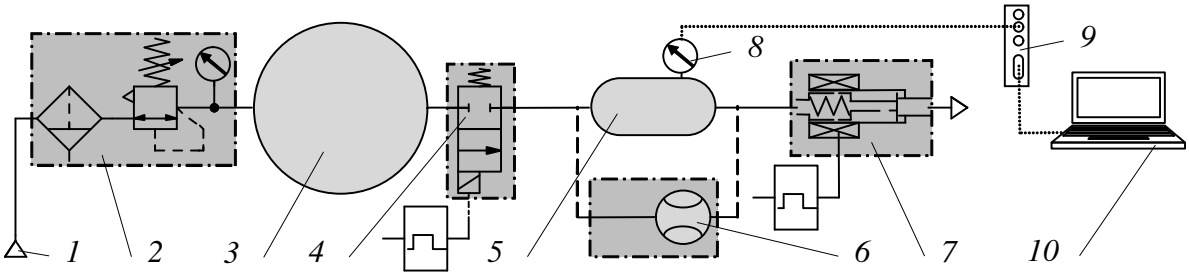

Fig. 2. **Structural schematics of the test stand (description in the main text)**

Parameters of the measurement equipment are presented in Table 2.

Table 2

Parameters of the measurement equipment

Parameter	Measurement device	Response time	Range (Accuracy)
Pressure	MPXH6400A	< 1 ms	(20-400)e3 Pa (±0.25 %)
Flow meter	BRONKHORST F-113AC-M50	< 2 s	(0-500) $l_n \cdot min^{-1}$ (±0.5 %)
Record	DAQ-6024E LabView – acquisition frequency of 1 ms using a DAQ-6024E measurement card (12 bit resolution) and the LabVIEW software bandwidth		

Results and discussion

In the static research, the plunger stroke was adjusted using the instrument presented in [36] (accuracy 0.01 mm). Every time the plunger stroke was set, the injector was mounted on a stand (Fig. 2) and the electronic system based on the STAG AC LLC gas controller forced the injector to open continuously. It was necessary to modulate the control signal using the PWM (Pulse-Width Modulation) to prevent the injector from overheating. The reading was made 5 s after the start of the measurements to include the response time of the flow meter. Measurements were repeated 3 times, the average values are presented in Fig. 3 (air pressure 1.25e5 Pa). The working range of the plunger stroke (0-0.4) mm was also determined.

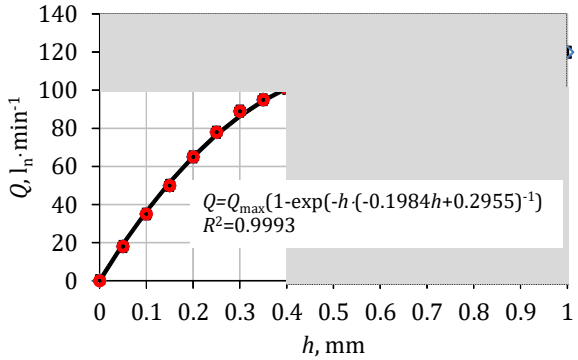

Fig. 3. **Flow characteristics of the research injector**

The volumetric flow rate Q value variability (Fig. 3) is described by a function characteristic for the first-order inertial object. The conformity of the experimental results with the approximation

function is visible, which is confirmed by the value of the coefficient of determination R^2 = 99.93%. Maximum value of the volumetric flow rate Q_{max} =120±2.5 $l_n \cdot min^{-1}$.

The flow through the opening injector valve (Fig. 3) can be divided into two phases. In the first one, a significant increase in the volumetric flow rate takes place, in the second one, a small one with a tendency to stabilise. As it can be observed in Fig. 3, the designers assume the opening range of the injector situated in the first phase. It is also a result of the necessity to obtain the appropriate opening and closing times to ensure proper cooperation with the engine control module. Stabilisation of the volumetric flow rate Q for the value of h > 0.8 mm was visible.

Evaluating the flow characteristics of the injector (Fig. 3), it can be observed that describing the flow area A as a proportion of the lift h, it was not able to represent the real process, even within the operating range of 0.4 mm. Therefore, a way of describing the flow capacity by determining the maximum value of the flow area A_{max} and considering the variability of the flow factor C was adopted.

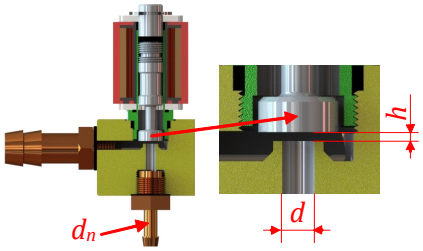

Fig. 4. **Dimensions of the injector valve**

In the investigated injector (Fig. 4), a nozzle with a diameter of d_n = 3.2 mm was mounted at the outlet and this value was taken as a representative for the calculation of the maximum flow area. When calculating the maximum value of the flow area A_{max} as the area of the injector outlet d = 4 mm and as the side wall of a cylinder with diameter d and height h = 1 mm, the same value of A_{max} = 12.57 mm^2 is obtained. In turn, by analysing the shape of the function in Fig. 3, a stabilisation for h > 0.8 mm is visible. It indicates that the flow is constrained by the nozzle diameter d_n. Therefore, the maximum flow area was finally calculated according to the nozzle diameter and it amounted to A_{max} = 8.04 mm^2, which is in compliance with the 0.8 mm high cylinder side wall.

Two methods were used to determine the flow factor value. In the first one the drag flow coefficient C_D value was calculated using the literature reports [37-40] (1):

$$C_D = \sqrt{\frac{1}{\frac{2\Delta p_{static}}{\rho}\left(\frac{\pi d_n}{4Q}\right)^2 + \left(\frac{d_n}{d_{upstream}}\right)^4}}, \quad (1)$$

where Δp_{static} – pressure decrease on the flow element, 1.25e5 Pa;
ρ – air density, 1.2 $kg \cdot m^{-3}$;
d_n – nozzle diameter, 3.2 mm;
Q – volumetric flow rate, $m^3 \cdot s^{-1}$;
$d_{upstream}$ – diameter of the preceding element, 6 mm.

In the second method, a dependence describing the mass flow of the air flowing through the pneumatic drag (in this case the gas injector) was used [32; 41; 42].

The basic simplifying assumptions of this model were:

- the air was regarded as a thermodynamically ideal gas (i.e. obeying the Clapeyron law), while being viscous and compressible;
- the flow takes place without internal friction and heat exchange with the surroundings;
- the state of the air is constant in a given volume and depends on time;
- the joints of the individual elements of the tested object are perfectly airtight;
- the air properties were assumed to be uniform both in the local volume and in the entire cross-section of the flow through the local resistance;
- the air temperature was constant in the process.

By transforming the dependence on the mass flow rate and considering air density at the volumetric flow rate, the flow factor C_f was determined [43] (2).

$$C_f = \frac{Q\rho}{A_{\max}\frac{p_t}{\sqrt{RT_t}}\psi_{\max} b\frac{p_t - p_t}{bp_t - p_a}} \tag{2}$$

where p_t – tank pressure, Pa;
R – gas constant, 287.15 J·kg^{-1}·K^{-1};
T_t – air temperature, 293.15 K;
$\psi_{\max}$ – max. value of the St` Venant and Wanzel function, 0.587;
b – factor of the Metlyuk-Avtushko function, 1.45;
p_a – atmospheric pressure, 1e5 Pa.

Calculated from equation (1) and (2), the C_D and C_f values indicated various maximum values (Fig. 5). In the case of the drag flow coefficient $C_{D\max} = 0.5384$, whereas the flow factor $C_{f\max} = 0.6772$, gives about 20% of the difference. Considering the fact that at a further stage the model description coinciding with the methodology of C_f determination was used, the flow factor was applied for the further analyses.

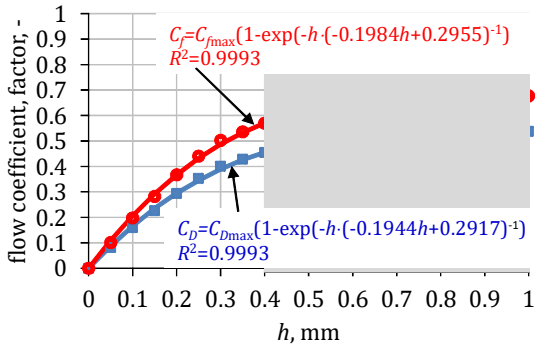

Fig. 5. **Calculated values of the flow coefficient/factor**

The differential equation describing the process of the air flow from the tank to the atmosphere through the local drag (taking into consideration the simplifying assumptions presented earlier) took the form (3):

$$\frac{dp_t}{dt} = -\frac{\kappa RT_t}{V_t}\left(C_f A_{\max}\right)\frac{p_t}{\sqrt{RT_t}}\psi_{\max} b\frac{p_t - p_t}{bp_t - p_a} \tag{3}$$

where V_t – volume of tank with pipe, 0.89e-3 m^3;
κ – adiabatic exponent, 1.4.

The value of the conductance ($C_f A_{\max}$) includes the constant maximum value of the flow area $A_{\max} = 8.04$ mm^2, and the variable value of the flow factor C_f described in the plunger lift function (4):

$$C_f = C_{f\max}\left(1 - \exp\left(\frac{-h}{-0.1984h + 0.2955}\right)\right) \tag{4}$$

The course of the injector opening (displacement h) was described basing on the results of the tests presented in [44; 45] in the absolute values of the dependence [46] (5):

$$\frac{h}{h_{\max}}(t) = \begin{cases} \frac{1}{t_o^2}t^2; & 0 \le t < 0 \\ 1; & t_o \le t < t_o + t_{fo} \\ -\frac{1}{t_c^2}t^2 + 1; & t_o + t_{fo} < t \le t_{inlet} \end{cases} \tag{5}$$

where t_o – opening time, 3.3 ms;

t_c – closing time, 2.2 ms;
t_{fo} – full open time, $t_{impulse} - t_o$ = 26.7 ms;
$t_{impulse}$ – impulse time, 30 ms;
t_{inlet} – inlet time, $t_{impulse} + t_c$ = 32.2 ms.

The validation was performed for 10 injector opening cycles with a frequency of 1000 min^{-1}. The initial condition of the pressure in both test variants was set to $p_{t\text{start}}$ = 1.25e5 Pa + p_a.

The simulations were carried out using the Matlab-Simulink environment. The differential equation (3) was solved numerically with the implicit trapezoidal method combined with reverse differentiation (time step 0.1 ms).

Experimental tests were performed on the test stand presented in Fig. 2, inducing a cyclic operation of the injector with STAG AC LLC system. Due to the long opening time, which was 30 ms, after 5 ms further power supply in the cycle was modulated with PWM signal.

Fig. 6 presents the input courses describing the operation of the injector in terms of one cycle, as well as 10 cycles, and a comparison of the pressure course in the tanks for the experimental and model variant. The conformity of the pressure courses is visible, which is evidenced by the percentage discrepancy graph, which values rarely exceed 0.5%.

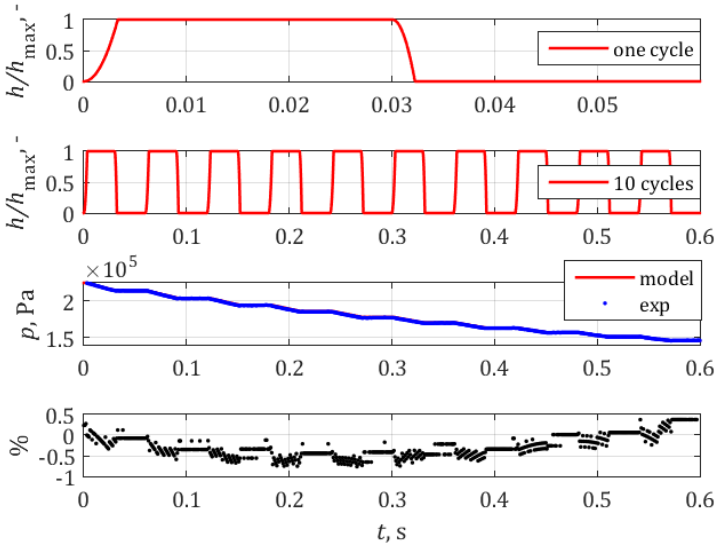

Fig. 6. **Results of the dynamic validation**

In the overall assessment of the validation two indicators were used – mean absolute percentage error (6):

$$MAPE = 100\left(MEAN \left| \frac{p_{t\,\mathrm{mod}} - p_{t\,\mathrm{exp}}}{p_{t\,\mathrm{exp}}} \right| \right), \ \% \tag{6}$$

and the maximum percentage error (7):

$$MaxPE = 100\left(MAX \left| \frac{p_{t\,\mathrm{mod}} - p_{t\,\mathrm{exp}}}{p_{t\,\mathrm{exp}}} \right| \right), \ \% \tag{7}$$

The values were respectively $MAPE$ = 0.33%, and $MaxPE$ = 0.76%, indicating the compatibility of the model course with the experimental. It demonstrated the correctness of the adopted methodology for determining the flow factor C_f for the gas injector valve and the possibility of applying it in the pulsating flow modelling. The occurring variations in the tank pressure courses are probably caused by the flow function adopted in the mathematical model. In the case of the mathematical descriptions presented in the article, the factor of the Metlyuk-Avtushko function was assumed at the level of 1.45, where originally it was 1.13. The difference results from the fact that the original value refers to continuous flows rather than the flows interfered by the impulse action of the gas injector.

Conclusions

1. The study presented the methodology of determining the flow factor for a low pressure gas injector.
2. In the first part, the plunger position was determined in a static method and the volumetric flow rate was determined. Determining the flow area allowed to determine the coefficient and flow factor. The maximum value of the drag flow coefficient was 0.5384, whereas the one of the flow factor was 0.6772, which gives about 20% difference.
3. Functions describing the coefficient and factor in relation to plunger elevation are presented, based on the first-order inertial object.
4. In the second part of the study, dynamic validation was conducted. Ultimately, model courses were compared with the experimental ones demonstrating the similarity, mean absolute percentage error did not exceed 0.5%.
5. The usefulness of the flow factor values obtained from static tests for the dynamic applications was proven.
6. The determined flow factor values can be used in the course of calculating the operation of the components of the alternative fuel supply of the combustion engines.

Funding

This publication was financed through the program of the Ministry of Science and Higher Education of Poland named “Regional Initiative of Excellence” in 2019-2022 project number 011/RID/2018/19.

Acknowledgements

This research was co-founded through the subsidy of the Ministry of Science and Higher Education for the discipline of Mechanical Engineering at the Faculty of Mechanical Engineering, Bialystok University of Technology.

References

[1] Reducing CO2 emissions from passenger cars. [online] [02.02.2020]. Available at: https://ec.europa.eu/clima/policies/transport/vehicles/cars_en.
[2] WLTP lab test. [online] [10.11.2019]. Available at: http://wltpfacts.eu/.
[3] Commission Regulation (EU) 2017/1154 of 7 June 2017 amending Regulation (EU) 2017/1151 supplementing Regulation (EC) No 715/2007 of the European Parliament and of the Council on type-approval of motor vehicles with respect to emissions from light passenger and commercial vehicles (Euro 5 and Euro 6) and on access to vehicle repair and maintenance information, amending Directive 2007/46/EC of the European Parliament and of the Council, Commission Regulation (EC) No 692/2008 and Commission Regulation (EU) No 1230/2012 and repealing Regulation (EC) No 692/2008 and Directive 2007/46/EC of the European Parliament and of the Council as regards real-driving emissions from light passenger and commercial vehicles (Euro 6). Official Journal of the European Union, L175, 7.7.2017, 708 p.
[4] Walus K.J., Wargula L., Krawiec P., Adamiec J.M. Legal regulations of restrictions of air pollution made by non-road mobile machinery - the case study for Europe: a review. Environmental Science and Pollution Research, vol. 25(4), 2018, pp. 3243-3259.
[5] Wargula L., Walus K.J., Krawiec P. Small engines spark ignited (SI) for non-road mobile machinery - review. Proceedings of 22nd International Scientific Conference “Transport Means 2018”, T.2, 2018, pp. 585-591.
[6] Onishi S., Jo S.H., Shoda K., Jo P.D., Kato S. Active thermo-atmosphere combustion (A.T.A.C.) - A new combustion process for internal combustion engines. SAE Paper, 790501, 1979.
[7] Jeuland N., Montagne X., Duret P. New HCCI/CAI combustion process development: Methodology for determination of relevant fuel parameters. Oil & Gas Science and Technology, vol. 59(6), 2004, pp. 571-579.
[8] Mikulski M., Balakrishnan P.R., Doosje E., Bekdemir C. Variable valve actuation strategies for better efficiency load range and thermal management in an RCCI engine. SAE Technical Papers, 2018-01-0254, 2018, 14 p.

[9] Fox J.T., Yang K., Hunsicker R. Diesel particulate filter cleaning effectiveness: estimated ash loading, quantified particulate removal, and post-cleaning filter pressure prop. Emission Control Science and Technology, 2019, pp. 1-11 (on-line).
[10] Senthil Kumar J., Ramesh Bapu B.R., Sivasaravanan S., Prabhu M., Abubacker M.A. Experimental studies on emission reduction in DI Diesel engine by using nano catalyst coated catalytic converter. International Journal of Ambient Energy, 2019, pp. 1-17 (on-line).
[11] Resitoglu I.A., Altinisik K., Keskin A., Ocakoglu K. The effects of Fe2O3 based DOC and SCR catalyst on the exhaust emissions of diesel engines. Fuel, vol. 262, 2020, 116501.
[12] Raslavicius L., Kersys A., Mockus S. Kersiene N., Starevicius M. Liquefied petroleum gas (LPG) as a medium-term option in the transition to sustainable fuels and transport. Renewable & Sustainable Energy Reviews, vol. 32, 2014, pp. 513-525.
[13] Borawski A. Modification of a fourth generation LPG installation improving the power supply to a spark ignition engine. Eksploatacja i Niezawodnosc - Maintenance and Reliability, vol. 17(1), 2015, pp. 1-6.
[14] Mikulski M., Wierzbicki S., Pietak A. Numerical studies on controlling gaseous fuel combustion by managing the combustion process of diesel pilot dose in a dual-fuel engine. Chemical and Process Engineering - Inzynieria Chemiczna i Procesowa, vol. 36 (2), 2015, pp. 225-238.
[15] Pulawski G., Szpica D. The modelling of operation of the compression ignition engine powered with diesel fuel with LPG admixture. Mechanika, vol. 21(6), 2015. pp. 501-506.
[16] Dimitrova Z., Marechal F. Gasoline hybrid pneumatic engine for efficient vehicle powertrain hybridization. Applied Energy, vol. 151, 2015, pp. 168-177.
[17] Raslavicius L., Kersys A. Makaras R. Management of hybrid powertrain dynamics and energy consumption for 2WD, 4WD, and HMMWV vehicles. Renewable and Sustainable Energy Reviews, vol. 68(1), 2017, pp. 380-396.
[18] Grigor'ev M.A., Naumovich N.I., Belousov E.V. A traction electric drive for electric cars. Russian Electrical Engineering, vol. 86(12), 2015, pp. 731-734.
[19] Simon M. Pneumatic vehicle, research and design. Procedia Engineering, vol. 181, 2017, pp. 200-205.
[20] Mathison S., Harty R., Cohen J., Gupta N., Sato H. Application of MC method-based H2 fueling. SAE Technical Paper 2012-01-1223, 2012, 12 p.
[21] Yangbo D., Xi J., Fengmin S. Combustion characteristics of advanced vortex combustor burning H2 fuel. ASME 2014 International Mechanical Engineering Congress and Exposition, V08AT10A013, 2014.
[22] Mieczkowski G. Description of stress fields and displacements at the tip of a rigid, flat inclusion located at interface using modified stress intensity factors. Mechanika vol. 21(2), 2015, pp. 91-98.
[23] Mieczkowski G. Stress fields at the tip of a sharp inclusion on the interface of a bimaterial. Mechanics of Composite Materials vol. 52(5), 2016, pp. 601-610.
[24] Mieczkowski G. Optimization and prediction of durability and utility features of three-layer piezoelectric transducers. Mechanika, vol. 24(3), 2018, pp. 335-342.
[25] Mieczkowski G., Borawski A., Szpica D. Static electromechanical characteristic of a three-layer circular piezoelectric transducer, Sensors, vol. 20, 2020, 222, 14 p.
[26] Borawski A. Common methods in analysing the tribological properties of brake pads and discs - a review. Acta Mechanica et Automatica, vol. 13(3), 2019, pp. 189-199.
[27] Borawski A. Suggested research method for testing selected tribological properties of friction components in vehicle braking systems. Acta Mechanica et Automatica, vol. 10(3), 2016, pp. 223-226.
[28] Grymek S., Kiczkowiak T. Conversion of the sonic conductance C and the critical pressure ratio b into the airflow coefficient μ. Journal of Mechanical Science and Technology vol. 19(9), 2005, pp. 1706-1710.
[29] Kaminski Z. Metody okreslania wlasciwości przepływowych elementow pneumatycznych, Hydraulika i Pneumatyka vol. 5, 2007, pp. 24-28. (In Polish).
[30] Valtek Type 30 – technical data. [online] [02.02.2020]. Available at: https://www.valtek.it/en/products/injectors/type-30.
[31] Szpica D. The influence of selected adjustment parameters on the operation of LPG vapor phase pulse injectors. Journal of Natural Gas Science and Engineering, vol. 34, 2016, pp. 127-1136.

[32] Szpica D. The determination of the flow characteristics of a low-pressure vapor-phase injector with a dynamic method. Flow Measurement and Instrumentation vol. 62, 2018, pp. 44-55.
[33] Kaminski Z. Ocena modeli matematycznych charakterystyk przeplywowych oporow pneumatycznych. Hydraulika i Pneumatyka vol. 5, 2003, pp. 1-4. (In Polish).
[34] Szpica D. Research on the influence of LPG/CNG injector outlet nozzle diameter on uneven fuel dosage. Transport, vol. 33(1), 2018, pp. 186-196.
[35] Rawski F., Szpica D. Identyfikacja parametrow modelu przepływu powietrza przez szczeline zaworowa w tlokowym silniku spalinowym. Motrol vol. 8, 2006, pp. 188-197. (In Polish).
[36] Szpica D. Testing the parameters of LPG injector solenoids as a function of the lift of the working component and the frequency of impulses. Proceedings of the 20th International Scientific Conference "Transport Means 2016", Kaunas University of Technology, Kaunas, Lithuania, pp. 551-555.
[37] Gamma Technologies Inc., GT-Suite Flow Theory Manual, 2012.
[38] Holmberg T., Cronhjort A., Stenlaas O. Pressure ratio influence on exhaust valve flow coefficients. SAE Technical Paper, 2017, 2017-01-0530.
[39] Semin S., Bakar R.A., Ismail A.R. Computational visualization and simulation of Diesel engines valve lift performance using CFD. American Journal of Applied Sciences vol. 5(5), 2008, pp. 532-539.
[40] Ariana M., Semin S., Kriswana D. Air flow and camshaft stress analysis of variable valve lift gas Engine. International Journal of Marine Engineering Innovation and Research, vol. 4(1), 2019 pp. 32-41
[41] Kaminski Z. Experimental and numerical studies of mechanical subsystem for simulation of agricultural trailer air braking systems. International Journal of Heavy Vehicle System, vol. 20(4), 2013, pp. 289-311.
[42] Kaminski Z. Mathematical modelling of the trailer brake control valve for simulation of the air brake system of farm tractors equipped with hydraulically actuated brakes. Eksploatacja i Niezawodnosc - Maintenance and Reliability, vol. 16(4), 2014, pp. 637-643.
[43] Xin Q. Diesel Engine System Design. First edition. Cambridge: Woodhead Publishing, 2013. 1088 p
[44] Duk M., Czarnigowski J. The method for indirect identification gas injector opening delay time. Przeglad Elektrotechniczny, vol. 88(10b), 2012, pp. 59-63.
[45] Czarnigowski J. Teoretyczno-empiryczne studium modelowania impulsowego wtryskiwacza gazu. Lublin: Politechnika Lubelska, 2012, 194 p. (In Polish).
[46] Szpica D., Korbut M. Modelling methodology of piston pneumatic air engine operation. Acta Mechanica et Automatica, vo. 13/4(50), 2019, pp. 271-278.